

# Detection of Myo-Inositol in-vivo using MR Chemical Exchange Saturation Transfer Imaging (MICEST)

M. Haris<sup>1</sup>, K. Cai<sup>1</sup>, A. Singh<sup>1</sup>, F. Kogan<sup>1</sup>, W. Witschey<sup>1</sup>, H. Hariharan<sup>1</sup>, and R. Reddy<sup>1</sup>  
<sup>1</sup>CMROI, Department of Radiology, University of Pennsylvania, Philadelphia, PA, United States

## INTRODUCTION

Myo-Inositol (MI) is one of the most abundant metabolites (~10mM) visible on proton magnetic resonance spectroscopy (<sup>1</sup>H MRS) of the human brain<sup>1</sup>. MI functions as an osmolyte and its concentration is altered in many brain disorders. MI has shown to be elevated in Alzheimer's disease, gliomatosis cerebri, renal failure, diabetes mellitus, recovering hypoxia, hyperosmolar states, and progressive multifocal leukoencephalopathy. MI has been found to be decreased in chronic hepatic and hypoxic encephalopathies, stroke, toxoplasmosis, cryptococcosis, lymphoma, and some low-grade malignancies. On MRS, MI is usually assigned to the aliphatic resonance peak present at 3.56ppm. The use of MRS to study MI is complicated by signal overlap due to the resonances of other key metabolites. While spectral editing techniques<sup>2</sup> have been proposed to edit the MI signal, <sup>1</sup>H MRS still lacks sufficient accuracy, is limited to low spatial resolution, and is time-consuming. Here, we describe a new, noninvasive, high resolution imaging technique for measuring MI. Development in this study is based on exploiting the hydroxyl proton groups on the MI molecule. The technique is based on the chemical exchange saturation transfer (CEST) where transfer of saturated magnetization from exchangeable protons leads to reduction in bulk water signal<sup>3</sup>. We demonstrate, for the first time, the high resolution spatial mapping of MI based CEST (MICEST) of labile protons (-OH) of MI with bulk water, in the human brain in-vivo.

## MATERIALS AND METHODS

**<sup>1</sup>H-Spectroscopy and Z-Spectrum of MI Exchangeable Protons:** Phantom of 10mM MI solution was prepared in phosphate buffered saline (PBS) and the pH was adjusted to 6.2 using 1N HCl/NaOH. <sup>1</sup>H-spectroscopy of both MI solutions and PBS (pH6.2) were acquired with water saturation. Another set of MI phantoms were prepared in PBS in concentrations of 1.0, 2.0, 5.0, 10.0 and 100mM. The pH of all solutions was adjusted to 7.4. Z-spectra from all samples were acquired over a frequency range of ±7.5ppm relative to the bulk water resonance in steps of 0.125ppm with a 1 second pre-saturation pulse of amplitude B<sub>1</sub>=127.8 Hz. These experiments were performed on a 9.4 T vertical bore scanner (Inova; Varian, Palo Alto, CA) using a 5-mm RF-probe.

**CEST Imaging:** MI solutions with different concentrations (1, 2, 5 and 10 mM, pH=7.4) were added to small test tubes (1.5cm diameter), and immersed inside a large beaker containing PBS. The CEST imaging was performed on a 7.0T Siemens whole-body clinical scanner (Siemens medical systems, Erlangen) using a transmit-receive head coil with a 1.5 second duration and 50 Hz amplitude pre-saturation RF pulse frequency selected +0.625ppm and -0.625ppm, followed by a gradient echo acquisition. The imaging parameters were: slice thickness=5mm, TR =7s, TE=3ms, field of view=240\*240 mm, matrix size=128\*128, and 32 echoes per TR. Using the same imaging parameters, MI CEST imaging was also performed on the brain of four normal volunteers (age: 27-35) with the same coil on the 7.0T Siemens scanner. B<sub>0</sub> and B<sub>1</sub> map of the same brain imaging slices were also obtained. The study was conducted under an approved Institutional Review Board protocol of the University of Pennsylvania. Informed consent from each volunteer was obtained after explaining the study protocol.

**CEST Image Processing:** CEST contrast was calculated by using the equation: CEST contrast = 100%\*[M<sub>neg</sub> - M<sub>pos</sub>] / M<sub>neg</sub>, where M<sub>pos</sub> and M<sub>neg</sub> are the acquired MR signals at +0.625ppm and -0.625ppm respectively. The CEST images were corrected for the B<sub>1</sub> and B<sub>0</sub> inhomogeneities.

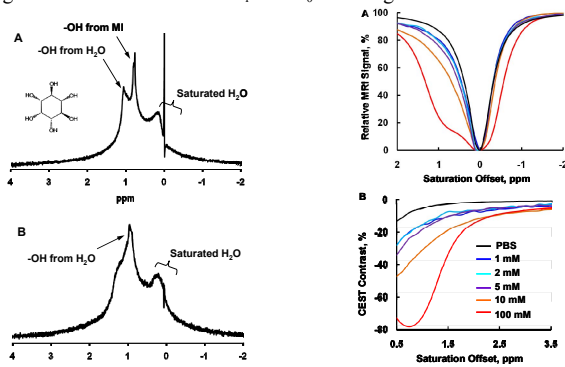


**Fig 1.** <sup>1</sup>H spectrum of MI (A) is showing the two -OH peaks at ~1ppm and ~0.6 ppm. PBS spectrum shows one -OH peak around ~1ppm (B).

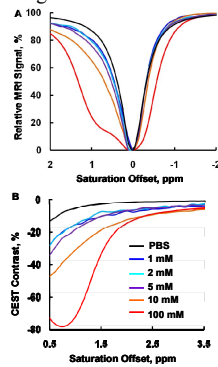


**Fig 2.** Z-spectra (A) of MI at different concentrations. Subtraction of Z-spectra shows the CEST effect at ~0.625ppm from the bulk water (B).

## RESULT AND DISCUSSION

**Phantom Studies:** High-resolution <sup>1</sup>H NMR spectra of MI (pH 6.2, 10 mM) and PBS (pH 6.2) are shown in Figure 1. The MI <sup>1</sup>H NMR spectrum showed two peaks at ~0.6ppm (~5.3ppm) and ~1ppm (~5.7ppm) downfield to the bulk water proton resonance. The PBS spectrum also showed one peak at ~5.7ppm. Based on this initial finding, we suggested that the peak present at ~5.7ppm is due to water -OH resonance while the peak at ~5.3ppm is due to MI -OH resonance. The MI Z-spectra showed a CEST peak at ~0.625ppm downfield of the bulk water resonance, demonstrating that the -OH peak at ~5.3ppm in the <sup>1</sup>H spectrum is the exchangeable group responsible for CEST effect. The PBS Z-spectra showed that there was no contribution of -OH resonance at ~5.7ppm to the CEST effect (Fig 2). Figure 3A demonstrates that the CEST effect increased with increasing MI concentration, indicating that the CEST effect of MI can serve as an index of its concentration based on a non-linear relationship. The graph shows that the MI CEST contrast varied from 6.6% (1mM) to 70% (10mM). CEST imaging of MI phantoms at varying concentrations (1, 2, 5 and 10mM) showed signal only from the inner chambers containing MI (Fig. 3B). No CEST contrast was observed from the outer chambers containing PBS. The MI CEST effect is unique in the sense that no other metabolites in the brain provide CEST contrast at this frequency (~0.625ppm). CEST effect observed from -OH protons of glucose shows negligible CEST effect around 2-3ppm at its physiological concentration (4.0mM)<sup>4,5</sup>. Only one CEST peak is observed from MI suggesting that all six -OH protons in MI resonate at the same frequency and contribute to the CEST effect. The presence of six exchangeable -OH protons in MI makes it a more appropriate endogenous CEST agent.

**In-vivo human brain imaging:** In the brain, a maximum MI CEST contrast of 55-60% was observed (Fig. 4). This is significant compared to any endogenous CEST contrast, and comparable to exogenous PARACEST agents. We selected a slice across the CSF to see if there is any asymmetric saturation. However, no asymmetric saturation was observed as the subtracted image showed no signal from the CSF. Low B<sub>1</sub> (<100 Hz) and long duration CEST imaging strategies has been proposed to minimize direction saturation<sup>6</sup>. In this study, we optimized very small B<sub>1</sub> (50Hz) and 1.5 seconds pulse duration for MICEST imaging. This method provides a noninvasive, and high spatial resolution imaging of MI in humans. The high resolution mapping of MI would be a major breakthrough to monitor different disease states, efficacy of treatment, and may provide a new disease biomarker in the future.

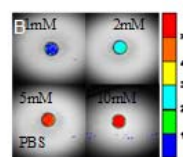
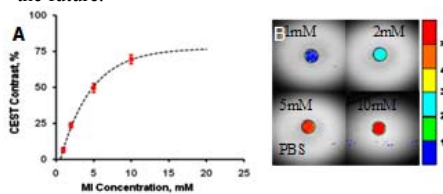


**Fig 3.** MI CEST contrast as a function of concentration (A). The CEST contrast was color-mapped and overlaid on the image obtained at -0.625ppm (B).

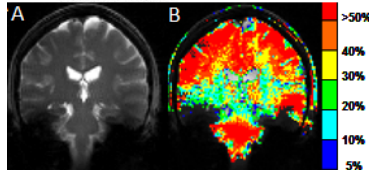


**Fig 4.** Coronal view of brain image and the corresponding CEST contrast map shows spatial distribution of MI in different region of brain (B).

**Acknowledgements:** This work was supported by Award Number P41RR002305 from the National Center for Research Resources.

**References 1:** Miller et al. Radiology 1993;187:433-437, 2: Kim et al. Magn Reson Med 2004;51:263-272, 3: Ward et al. J Magn Reson. 2000;143:79-87, 4: van Zijl PC et al. Proc Natl Acad Sci U S A. 2007;104:4359-64, 5: Criego et al. J Neurosci Res. 2005;82:525-30, 6: Sun et al. J Magn Reson. 2005;175:193-200.